Published in final edited form as:
Exp Neurol. 2010 October ; 225(2): 341–352. doi:10.1016/j.expneurol.2010.07.005.

Intravenous multipotent adult progenitor cell therapy for traumatic brain injury: Preserving the blood brain barrier via an interaction with splenocytes

Peter A. Walker, MD[1,2], **Shinil K. Shah, DO**[1,2,4], **Fernando Jimenez, MS**[2], **Michael H. Gerber, BS**[1,3], **Hasen Xue, MD**[1,2], **Rochelle Cutrone, MS**[5], **Jason A. Hamilton, PhD**[5], **Robert W. Mays, PhD**[5], **Robert Deans, PhD**[5], **Shibani Pati, MD, PhD**[1], **Pramod K Dash, PhD**[3], and **Charles S. Cox Jr., MD**[1,2,4]

[1]Department of Surgery, University of Texas Medical School at Houston, Houston, Texas

[2]Department of Pediatric Surgery, University of Texas Medical School at Houston, Houston, Texas

[3]Department of Neurobiology and Anatomy, University of Texas Medical School at Houston, Houston, Texas

[4]the Michael E DeBakey Institute for Comparative Cardiovascular Science and Biomedical Devices, Cleveland, Ohio

[5]Texas A & M University, College Station, Texas, and Department of Regenerative Medicine, Athersys Inc., Cleveland, Ohio

Abstract

Recent investigation has shown an interaction between transplanted progenitor cells and resident splenocytes leading to modulation of the immunologic response in neurological injury. We hypothesize that the intravenous injection of multipotent adult progenitor cells (MAPC) confers neurovascular protection after traumatic brain injury through an interaction with resident splenocytes, subsequently leading to preservation of the blood brain barrier.

Four groups of rats underwent controlled cortical impact injury (3 groups) or sham injury (1 group). MAPC were injected via the tail vein at two doses ($2*10^6$ MAPC/kg or $10*10^6$ MAPC/kg) 2 and 24 hours after injury. Blood brain barrier permeability was assessed by measuring Evans blue dye extravasation (n=6/group). Additionally, splenic mass was measured (n=12/group) followed by splenocyte characterization (n=9/group) including: cell cycle analysis (n=6/group), apoptosis index (n=6/group), cell proliferation (n=6/group), and inflammatory cytokine measurements (n=6/group). Vascular architecture was determined by immunohistochemistry (n=3/group).

Traumatic brain injury results in a decrease in splenic mass and increased blood brain barrier permeability. Intravenous infusion of MAPC preserved splenic mass and returned blood brain

Address inquiries to: Charles S. Cox, Jr, MD, Department of Pediatric Surgery, University of Texas Medical School at Houston, 6431 Fannin Street, MSB 5.236, Houston, Texas, 77030, Phone: 713-500-7307; Fax: 713-500-7296, Charles.s.cox@uth.tmc.edu.

Conflict Statement: There are no known conflicts between the authors and the information presented in this paper. Charles S. Cox Jr., MD has sponsored research agreements with Athersys, Inc. and Cord Blood Registry, Inc.

barrier permeability towards control sham injured levels. Splenocyte characterization indicated an increase in the number and proliferative rate of CD4+ T cells as well as an increase in IL-4 and IL-10 production in stimulated splenocytes isolated from the MAPC treatment groups. Immunohistochemistry demonstrated stabilization of the vascular architecture in the peri-lesion area

Traumatic brain injury causes a reduction in splenic mass that correlates with an increase in circulating immune cells leading to increased blood brain barrier permeability. The intravenous injection of MAPC preserves splenic mass and the integrity of the blood brain barrier. Furthermore, the co-localization of transplanted MAPC and resident CD4+ splenocytes is associated with a global increase in IL-4 and IL-10 production and stabilization of the cerebral microvasculature tight junction proteins.

MeSH Keywords

Multipotent adult progenitor cells; traumatic brain injury; stem cells; splenocytes; blood brain barrier

Introduction

Traumatic brain injury (TBI) affects 1.5 million people in the United States annually with an associated mortality of 50,000 (Thurman, et al., 1999). Furthermore, the long term cognitive, psychosocial, and physical deficits associated with TBI (1999) lead to an annual economic impact of 60 billion dollars (Faul, et al., 2007, Walker, et al., 2009).

Mesenchymal stromal cells (MSCs) have shown promise as a novel therapy for multiple central nervous system pathologies (Liao, et al., 2009, Lim, et al., 2007, Qu, et al., 2008). While initial *in vivo* research suggested that MSCs engrafted at the site of injury with possible differentiation into neuronal cells (Deng, et al., 2006, Zhao, et al., 2002), the importance of engraftment and frequency of transdifferentiation remains controversial (Castro, et al., 2002, English, et al., 2006, Walker, et al., 2009).

Multipotent adult progenitor cells (MAPC) are a more primitive form of bone marrow derived progenitor cells that have been shown to differentiate into mesodermal, neuroectodermal, and endodermal cell types (Jiang, et al., 2002). Fischer et al have shown that up to twice as many MAPC bypass the pulmonary capillary bed compared to the larger MSCs after intravenous injection, leading to an increased volume of cells in contact with splenocytes (Fischer, et al., 2009). The observed suitability of MAPC to achieve early “off the shelf” dosing and the ability to decrease the observed first pass pulmonary effect make MAPC an attractive candidate for novel progenitor cell therapy.

TBI, like ischemic stroke, stimulates adrenergic output that leads to the release of immune cells derived from the spleen ultimately leading to a loss of splenic mass (Ajmo, et al., 2009, Cotton, et al., 2007) The pro-inflammatory environment after TBI leads to breakdown of the blood brain barrier (BBB) thereby worsening the deficit associated with injury. After intravenous injection in a TBI model, MAPC come into contact with many organ systems including the spleen. We hypothesized that intravenous MAPC injection would preserve (Vendrame, et al., 2006) the lost splenic mass and potentially increase splenocyte proliferation resulting in production of anti-inflammatory cytokines such as IL-4 and IL-10. The production of IL-4/IL-10 could modulate the pro-inflammatory response after injury in the direct injury and penumbral regions of the brain leading to preservation of the BBB. To test our hypothesis, a series of *in vivo* and *in vitro* experiments were completed to investigate the interaction of intravenous MAPC therapy with splenocytes and their resultant

effect on the BBB. Figure 1 outlines the experimental design constructed to test our hypothesis.

Methods

All protocols involving the use of animals were in compliance with the National Institutes of Health *Guide for the Care and Use of Laboratory Animals* and were approved by the University of Texas Institutional Animal Care and Use Committee (protocol HSC-AWC-08-156).

In vivo methods

Controlled cortical impact injury—A controlled cortical impact (CCI) device (eCCI Model 6.3; VCU, Richmond, VA)) was used to administer a unilateral brain injury as described previously (Lighthall, 1988). Male rats weighing 225 – 250 gram were anesthetized with 4% isoflurane and O_2 and the head was mounted in a stereotactic frame. The head was held in a horizontal plane, a midline incision used for exposure, and a 7-8 mm craniectomy was performed on the right cranial vault. The center of the craniectomy was placed at the midpoint between bregma and lambda, ~3 mm lateral to the midline, overlying the tempoparietal cortex. Animals received a single impact of 3.1 mm depth of deformation with an impact velocity of 5.8 m/s and a dwell time of 150 ms (moderate-severe injury) at an angle of 10° from th e vertical plane using a 6 mm diameter impactor tip, making the impact orthogonal to the surface of the cortex. The impact was made to the parietal association cortex. Sham injuries were performed by anesthetizing the animals, making the midline incision, and separating the skin, connective tissue, and aponeurosis from the cranium. The incision was then closed (Harting, et al., 2008).

Preparation and intravenous injection of MAPC—MAPC were obtained from Athersys, Inc. (Cleveland, OH) and stored in liquid nitrogen. Prior to injection, the MAPC were thawed, washed and suspended in phosphate buffered saline (PBS) vehicle at a concentration of $2 * 10^6$ cells/mL. Cells were counted and checked for viability via Trypan blue exclusion. Immediately prior to intravenous injection, MAPC were titrated gently 8–10 times to ensure a homogeneous mixture of cells. MAPC were injected at both 2 and 24 hours after CCI injury at 2 different dosages (CCI + $2 * 10^6$ MAPC/kg, and CCI + $10 * 10^6$ MAPC/kg). Therefore, each treatment animal received 2 separate doses of their assigned MAPC concentration. CCI injury control animals received PBS vehicle injection alone at the same designated time points as the cell treated animals

Rat splenectomy—For all experiments completed with rats after splenectomy, male sprague dawley rats were obtained from Harlon Inc. According to the supplier, the animals were anesthetized as described above and placed in the supine position. A small 3 cm incision was made in the left upper quadrant of the abdomen followed by retraction of the spleen and ligation of the splenic hilum. After removal of the spleen the incision was closed with a running suture. Our laboratory received the animals 48 hours after splenectomy and allowed the animals to further recover and acclimate for 24 hours. All experiments were then completed 72 hours after the original splenectomy.

Evan's blue BBB permeability analysis—Seventy two hours after CCI injury, the rats were anesthetized as described above, and 1 mL (4cc/kg) of 3% Evan's blue dye in PBS was injected via direct cannulation of the right internal jugular vein. The animals were allowed to recover for 60 minutes to allow for perfusion of the dye. After this time, the animals were sacrificed via right atrial puncture and perfused with 4% paraformaldehyde. Next, the animals were decapitated followed by brain extraction. The cerebellum was dissected away

from the rest of the cortical tissue. The brain was divided through the midline and the mass of each hemisphere (ipsilateral to injury and contralateral to injury) was measured for normalization. Subsequently, each hemisphere was allowed to incubate overnight in 5 mL of formamide (Sigma Aldrich, St. Louis, MO) at 50 degrees centigrade to allow for dye extraction. After centrifugation, 100 μL of the supernatant from each sample was transferred to a 96 well plate (in triplicate) and absorbance was measured at 620 nm using the VersaMax plate reader (Molecular Devices Inc., Sunnyvale, CA). All values were normalized to hemisphere weight.

Cortical immunohistochemistry—Seventy two hours after CCI injury, 4 groups (uninjured, CCI injury alone, CCI injury + 2 * 10^6 MAPC/kg, and CCI injury + 10 * 10^6 MAPC/kg) of both rats with intact spleens and rats after splenectomy were sacrificed followed quickly by decapitation. Of note, animals were allowed to recover for 72 hours after splenectomy prior to CCI injury. The brains were extracted and both hemispheres (ipsilateral and contralateral to injury) were isolated. The tissue samples were then quickly placed into pre-cooled 2-methylbutane for flash freezing. The samples were transferred to dry ice and stored at -80 degrees centigrade until the tissue was sectioned.

Next the tissue samples were placed in Optimal Cutting Temperature compound (Sakura Finetek, Torrance, CA) and 20 μm cryosections were made through the direct injury area. Direct injury to the vascular architecture was evaluated via staining with an antibody for the tight junction protein occludin (1:150 dilution, Invitrogen, Carlsbad, CA) and appropriate fluoroescein isothiocyanate (FITC) conjugated secondary antibody (1:200 dilution, Invitrogen, Carlsbad, CA). After all antibody staining, the tissue sections were counterstained with 4′6-diamidino-2-phenylindole (DAPI) (Invitrogen, Carlsbad, CA) for nuclear staining and visualized with fluorescent microscopy.

Splenic immunohistochemistry—In order to track MAPC *in vivo*, 4 groups of rats (uninjured, CCI injury alone, CCI injury + 2 * 10^6 MAPC/kg, and CCI injury + 10 * 10^6 MAPC/kg) underwent either sham injury or CCI injury. Next, the two treatment groups received injections of quantum dot (QDOT, Qtracker cell labeling kit 525 and 800, Invitrogen, Inc., Carlsbad, CA) labeled (per manufacturer's suggested protocol) MAPC, 2 and 24 hours after CCI injury. Six hours after the second QDOT labeled MAPC infusion, the animals were sacrificed and the spleens removed. Tthe spleens were subsequently placed on a fluorescent scanner (Odyssey Imaging System, Licor Inc., Lincoln, NE) to localize QDOT labeled MAPC. After the scan was completed, the tissue samples were then quickly placed into pre-cooled 2-methylbutane for flash freezing. The samples were transferred to dry ice and stored at -80 degrees centigrade until use.

Next the tissue samples were placed in Optimal Cutting Temperature compound (Sakura Finetek,Torrance, CA) and 10 μm cryosections were made through the spleens. The tissue sections were stained with 4′6-diamidino-2-phenylindole (DAPI) (Invitrogen, Carlsbad, CA) for nuclear staining and both the QDOT labeled MAPC and splenocytes were visualized with fluorescent microscopy. Furthermore, hematoxylin and eosin staining (Sigma Aldrich, Inc, St. Louis, MO) was completed per manufacturer's suggested protocol to evaluate splenic architecture.

Splenocyte isolation—Seventy two hours after injury, the animals underwent splenectomy with measurement of splenic mass. Of note the animals were euthanized at this time. Next, the spleens were morselized using a razor blade, washed with basic media (10% FBS and 1% penicillin/streptomycin in RPMI), crushed, and filtered through a 100 μm filter. The effluent sample from the filter was gently titrated 8-10 times and subsequently filtered through a 40 μm filter to remove any remaining connective tissue. The samples were

centrifuged at 1000 g for 3 minutes. Next the supernatant solutions were removed and the samples were suspended in 3 mL of red blood cell lysis buffer (Qiagen Sciences, Valencia, CA) and allowed to incubate on ice for 5 minutes. Subsequently, the samples were washed twice with basic media and centrifuged using the aforementioned settings. The splenocytes were counted and checked for viability via Trypan blue exclusion.

***In vivo* splenocyte proliferation assay—**The percentage of actively proliferating splenocytes (S phase) after at the time of sacrifice was measured using Click-iT™ EdU Flow Cytometry Assay Kit (Invitrogen, Carlsbad, CA). The manufacturer's suggested protocol was followed. Briefly, splenocytes were harvested at 72 hours as previously described. At this point 20 mM of EdU was added and allowed to incubate for 2 hours. Next, the cells were washed and fixed with 4% paraformaldehyde. Cells were permeablilized using Triton-X100 and then the anti-EdU antibody “cocktail” provided by the manufacturer was added. Finally, the cells were washed followed by the addition of Ribonuclease and CellCycle488-Red stain to analyze DNA content. We collected 10,000 events per analysis.

***In vivo* splenocyte apoptosis assay—**The percentage of apoptotic splenocytes at the time of sacrifice was measured using an Annexin V stain (BD Biosciences, San Jose, CA). The manufacturer's suggested protocol was followed. Briefly, after isolation, splenocytes were washed twice with cold PBS. Next $1 * 10^6$ cells were incubated with 5 μL of Annexin V and 7-Amino-Actinomycin (7-AAD) for 15 minutes. At this time flow cytometry was used to measure the percentage of apoptotic cells. We collected 10,000 events per analysis.

Quantitative PCR—RNA was isolated from splenocytes using RNEasy columns (Qiagen, Valencia, CA) according to manufacturer's specifications. Rat reference RNA (Stratagene, La Jolla, CA) was used as a positive control. Synthesis of cDNA was performed with M-MLV reverse transcriptase and random hexamers (Promega, Madison, WI). Control reactions were performed without reverse transcriptase to control for genomic DNA contamination. SYBR Green quantitative PCR was performed using the primers listed in Table 1. qPCR was performed using an ABI 7500 with 9600 emulation. The PCR conditions were 50°C × 2 min, 95°C × 10 min, and then 40 cycles of 95°C × 15 sec, 60°C × 1 min. Values were normalized to β-actin and expressed as relative fold change compared to sham control animals.

In vitro

Splenocyte culture—Splenocytes cultured at a density of $7.5 * 10^5$ cells/mL were then allowed to expand for 72 hours in growth media (10% FBS, 1% RPMI with vitamins, 1% sodium pyruvate, 0.09% 2-mercaptoethanol, and 1% penicillin/streptomycin in RPMI) stimulated with 2 μg concanavalin A.

Splenocyte characterization—The isolated splenocytes were analyzed with flow cytometry (LSR II, BD Biosciences, San Jose, CA) to determine the monocyte, neutrophil, and T cell populations. Monocytes and neutrophils were measured using antibodies to CD200 (Abcam, Cambridge, MA) and CD11b/CD18 (Abcam, Cambridge, MA), respectively. The splenocyte T cell populations were labeled using CD3, CD4, and CD8 antibodies (Abcam, Cambridge, MA). All staining was completed in accordance with manufacturer's suggested protocol. Of note, the T cell populations of interest were CD3+/CD4+ and CD3+/CD8+. We acquired 10,000 events for each gated cell population.

Proliferation assay *in vitro*—The percentage of CD4+ splenocytes actively proliferating (S phase) after culture in stimulated growth media was measured using Click-iT™ EdU

Flow Cytometry Assay Kit (Invitrogen, Carlsbad, CA). The manufacturer's suggested protocol was followed. Briefly, splenocytes were cultured for 72 hours as previously described in growth media stimulated with 2 μg concanavalin A at a density of $7.5 * 10^5$ cells/mL. At this point 20 mM of EdU was added and allowed to incubate for 1 hour. Next, the cells were washed with 4% bovine serum in DMEM (4% FBS) and CD4-PE (Biolegend Inc., San Diego, CA) was added to gate the T cell population of interest. After 30 minutes of incubation, the cells were washed and fixed with 4% paraformaldehyde. Cells were permeablilized using Triton-X100 and then the anti-EdU antibody "cocktail" provided by the manufacturer was added. Finally, the cells were washed followed by the addition of Ribonuclease and CellCycle488-Red stain to analyze DNA content. We gated on the CD4+ cells and collected 10,000 events per analysis.

Splenocyte cytokine production *in vitro*—After culture in stimulated growth media, production of the anti-inflammatory cytokines IL-4 and IL-10 was quantified by flow cytometry using a BD Cytometric Bead Array flex set (BD Biosciences, San Jose, CA) following manufacturer's suggested protocol. A BD LSR II flow cytometer containing the FCAP Array ™ software was used to analyze our samples.

Data Analysis—Unless otherwise indicated, all values are represented as mean ± SEM. Values were compared using analysis of variance (ANOVA) with a post-hoc Tukey analysis. A p value of ≤0.05 was used to denote statistical significance.

Results

Blood brain barrier (BBB) permeability

BBB permeability measurements were completed using Evan's blue dye in both TBI injured sham splectomized rats and TBI injured/splectomized rats (n = 6/group). Figure 2 shows the mean absorbance (nm) normalized to tissue weight (grams) derived from homogenized cortical tissue derived from the hemisphere ipsilateral to the CCI injury. TBI injured/sham splectomized rats show a significant increase in BBB permeability after injury (p = 0.0001) that is reversed by the intravenous injection of MAPC. Furthermore, TBI injured rats receiving splenectomy fail to show such a dramatic increase in permeability. It is important to note that the MAPC mediated effect is dependent upon an intact spleen and is equivalent for both the lower and higher cell dosage.

Tight junction immunohistochemistry

BBB integrity was further examined by immunostaining for the tight junction protein, occludin, and visualization with fluorescent microscopy (DAPI blue for nuclei and FITC green for occludin) (n =3/group). Figure 3 shows representative images from each group for rats with intact spleens (uninjured, CCI injury alone, CCI + $2 * 10^6$ MAPC/kg, and CCI + $10 * 10^6$ MAPC/kg). There is a qualitative decrease in occludin staining in the CCI injury control animals when compared to the uninjured control group. Additionally, there is a qualitative increase in occludin observed for both treatment groups. Close observation of the CCI + $2 * 10^6$ MAPC/kg treatment group shows an increased occludin signal likely due to decreased breakdown of the tight junctions; however, the vasculature appears to be shorter and more disorganized than the uninjured animals. Furthermore, qualitative analysis of the CCI + $10 * 10^6$ MAPC/kg treatment groups suggests both increased occludin staining and a larger population of more lengthy and organized vessels.

Analysis of the tight junction protein, occludin, was repeated with rats after splenectomy and representative images are shown in figure 4. Observation of the images shows a decrease in occludin staining in the CCI injury control and treatment animals when compared to the

uninjured control group. The observed difference is less pronounced than in the normal rats. Additionally, no clear difference in occludin staining is observed between the CCI injury alone and treatment groups.

Splenic mass

Seventy two hours after CCI injury, rats (n = 12/group) were sacrificed and splenic mass measured (Figure 5A). A significant decrease in mass (p = 0.002) is observed in the CCI alone control animals (0.62 ±0.014 grams) when compared to uninjured controls (0.76 ±0.029 grams). In addition, the splenic mass was preserved administration of MAPC at both dose tiers: $2 * 10^6$ MAPC/kg (0.74 ±0.037 grams) and $10 * 10^6$ MAPC/kg (0.75 ±0.026 grams).

Splenocyte characterization

Splenocytes were isolated 72 hours after CCI injury for characterization using flow cytometry (n = 9/group). Figure 5B outlines the percentage of splenocytes that were CD3+/CD4+ or CD3+/CD8+ double positive as well as the CD8+/CD4+ ratio. A trend towards increased CD3+/CD4+ double positive cells was observed at the $2 * 10^6$ MAPC/kg cell dosage that reaches significance at the higher ($10 * 10^6$ MAPC/kg) cell dosage ($p < 0.001$). No difference in CD3+/CD8+ double positive cells was observed. Furthermore, no difference in the CD8+/CD4+ ratio was observed.

In addition to T cell characterization, the splenocytes were stained with CD200 and CD11/CD18b to measure the monocyte and neutrophil populations, respectively (n = 3/group). There was no significant differences that were noted between the groups (data not shown).

In vivo MAPC tracking

In order to ensure that MAPC were bypassing the pulmonary microvasculature and reaching the spleen, quantum dot labeled MAPCs were injected (n =2/group). Six hours after the second cell dose a splenectomy was performed. Figure 6A shows a fluorescent scan of both total splenic body and splenic cross section to display the amount of MAPC located in the spleen. As expected, no signal (blue) is observed in the CCI injury alone control group. Further observation shows increasing signal (yellow representing a moderate signal and red representing a high signal level) for both of the treatment groups indicating an increasing number of MAPC located within the splenic tissue as a function of increasing dose.

To further investigate the location of MAPC within the splenic tissue, structural staining and immunofluorescence were completed as previously described. Figure 6 B-C shows a structural H & E stain of a splenic cross section. Both images show a perforating arteriole within the splenic tissue. It is important to note that the splenic white pulp (areas rich in lymphocytes) are located around the arterioles. Furthermore, figure 6 D-E shows quantum dot labeled MAPC (labeled green) located within the white pulp in close approximation with the blood vessel, suggesting an interaction with the resident splenic lymphocyte population.

Splenocyte proliferation

Measurement of splenocyte proliferation was completed via 2 separate assays (n = 6/group). Immediately after sacrifice, cell cycle analysis was completed using a Click It Edu kit (Invitrogen, Carlsbad, CA) as previously described. Figure 7A shows a significant increase in splenocyte proliferation at the higher MAPC dose (1.30 +/− 0.21%) when compared to CCI injury control animals (0.60 +/− 0.08%) (p = 0.002). In addition, qPCR was completed to measure the expression of the proliferative genes Cdc 20 and Cdc 2a. Figures 7B-C show significant increases in Cdc 20 expression for both treatment groups (p = 0.01) and in Cdc 2a expression for the higher ($10 * 10^6$ MAPC/kg) treatment group (p = 0.03) when

compared to CCI injury controls. Values are expressed as fold increase from uninjured controls which are set to a value of 1.

Splenocyte apoptosis

Measurement of splenocyte apoptosis was completed via 2 separate assays (n = 6/group). Immediately after sacrifice, cell cycle analysis was completed using a Annexin V stain (BD Biosciences, San Jose, CA) as previously described. Figure 8A shows a significant decrease in splenocyte apoptosis at the higher MAPC dose (2.00 +/− 0.33%) when compared to CCI injury control animals (3.57 +/− 0.38%) ($p = 0.03$). In addition, qPCR was completed to measure the expression of the apoptosis genes caspase 7 and caspase 12. Figure 8B shows a decrease in caspase 12 expression for the higher ($10 * 10^6$ MAPC/kg) treatment group ($p < 0.001$) when compared to CCI injury controls. Figure 8C shows a trend towards decreased caspase 7 expression for both treatment groups that fails to reach significance by post hoc analysis ($p = 0.02$). Values are expressed as fold increase from uninjured controls which are set to a value of 1.

Pro and anti inflammatory cytokine measurement *in vivo*

Splenocyte pro and anti inflammatory cytokine production was measured *in vivo* via completion of qPCR for inteferon gamma (IFNγ), interleukin 6 (IL-6), and interleukin 10 (IL-10) (n = 6/group). Figure 9A shows a significant increase in anti inflammatory cytokine (IL-10) production at the higher MAPC dose ($10 * 10^6$ MAPC/kg) when compared to CCI injury control animals ($p = 0.006$). Figures 9 B-C show a decrease in production of the pro inflammatory cytokines IL-6 and IFNγ that fails to reach significance ($p = 0.07$ and $p = 0.14$, respectively). Values are expressed as fold increase from uninjured controls which are set to a value of 1.

CD4+ T cell proliferation *in vitro*

To further investigate the significant increase in CD4+ T cells observed *in vivo*, cell cycle analysis was completed using a flow cytometric based BRDU assay kit (n = 6/group) on stimulated splenocyte cultures. Splenocytes were gated for CD4+ and then the percentage of cells in S phase (actively proliferating) was measured. Figure 10A shows a decrease in CD4+ S phase proliferation observed for the CCI injury alone control animals (27.7 ±6.6 %) compared to the uninjured controls (43.8 ±1.9 %). In addition, the proliferative rate was restored by injection at both $2 * 10^6$ MAPC/kg (46.2 ±2.6 %) and $10 * 10^6$ MAPC/kg (45.9 ±3.5 %) cell dosages ($p = 0.01$).

In vitro anti inflammatory cytokine production

The potential effect of MAPC therapy on the systemic inflammatory response was tested as splenocytes were isolated and cultured in stimulated growth media as described above. Using a flow cytometry bead based cytokine array, the production of the anti inflammatory cytokines IL-4 and IL-10 (pg/ml) was measured and are displayed in Figure 10B. A trend towards increased IL-4 and IL-10 production is observed for both treatment groups compared to CCI injury alone control animals. This is significant at the higher cell dosage ($10 * 10^6$ MAPC/kg) for both IL-4 ($p = 0.02$) and IL-10 ($p = 0.03$) production.

Discussion

Our data show that CCI injury results in a decreased splenic mass and an increase in BBB permeability. Intravenous MAPC therapy preserved splenic mass and returned BBB permeability towards sham levels at both cell dosages. The same protocol completed in rats after splenectomy failed to demonstrate a dramatic increase in BBB permeability with CCI

injury and showed no difference between control and cell treated groups. Therefore, the observed cell benefit required an interaction between injected MAPC and resident splenocytes. At the time of harvest, a decrease in splenocyte apoptosis with concordant increase in proliferation was observed. Quantitative PCR showed an increase in IL-10 production *in vivo* without a significant decrease in IFNγ or IL-6 production. Characterization of splenocyte cultures showed an increase in the absolute number and proliferative rate of CD4+ T cells as well as an increase in IL-4 and IL-10 production in stimulated splenocytes isolated from the MAPC treatment groups. Immunohistochemistry demonstrated stabilization of the vascular architecture in the peri-lesion area. Figure 11 outlines our proposed mechanism of MAPC therapy leading to preservation of the BBB barrier in TBI.

Initial investigation into the role of mesenchymal stromal cell (MSCs) therapeutics for TBI indicated that MSC migration to the site of injury, engraftment, and transdifferentiation could be potential mechanisms for restoration of function(Deng, et al., 2006); however, the frequency of engraftment and effect of transdifferentiation remains highly controversial. Additionally, many investigators have failed to replicate the early cognitive improvement observed in pre clinical animal models (Harting, et al., 2009).

The notion that intravenous injected therapeutic cells must reach the site of injury for effect faces a substantial barrier with the significant first pass pulmonary effect due to the sequestration of MSCs (diameter 15 – 19 μm) in the pulmonary capillaries (Fischer, et al., 2009, Harting, et al., 2008). The intravenous injection of labeled 4, 10, and 15 μm microspheres followed by lung tissue harvest showed no 4 μm microspheres in the lung tissue; however, 10 and 15 μm microspheres were sequestered in the capillary beds. These data support the conclusion that the average pulmonary capillary diameter is functionally 5 – 9 μm correlating closely with anatomic measurements and explaining the inability of MSCs to bypass the lungs (Schrepfer, et al., 2007).

Fischer et al have shown that the vast majority of MSCs are sequestered in the lungs after intravenous injection (Fischer, et al., 2009). Such an effect decreases the number of cells reaching the site of injury/parenchyma. While it is possible that only a few MSCs need to reach the site of injury for effect, an alternative hypothesis is that the cells are interacting with distant organ systems such as lung tissue or the reticuloendothelial system to generate an alteration in the systemic inflammatory/immunologic response. An obvious method to enhance progenitor cell delivery to the site of action would be to use cells with a smaller diameter which could more readily bypass the pulmonary capillary beds. MAPC are a more primitive progenitor cell line with a smaller diameter then MSCs (Boozer S, 2009). Fischer et al. have shown that 2-fold as many MAPC are able to bypass the pulmonary capillary beds (compared to MSCs) and potentially reach distant sites of action(Fischer, et al., 2009) making MAPC an attractive candidate for novel cell based therapeutics.

Previous work completed by Offner et al. have shown ischemic stroke to be associated with the loss of splenocytes in accordance with an increase in TUNEL+ apoptotic cells within the spleen, leading to decreased T cell proliferation and cytokine production causing a state of immunosuppression after stroke (Offner, et al., 2006). Separate experiments completed by Offner et al. have shown a peripheral increase in production of the pro inflammatory cytokines TNFα, IFNγ, IL-6, MCP-1, and IL-2 after ischemic stroke (Offner, et al., 2006). Further work completed by Ajmo et al. has shown that ischemic stroke is associated with adrenergic output that stimulates the spleen to release immune (T and B cells) into the systemic circulation that ultimately lead to increased cavity size after MCAO stroke in a rodent model (Ajmo, et al., 2009). Furthermore, Verdrame et al. have shown similar results indicating the release of immune cells (CD8+ T cells) is correlated with a reduction in

splenic mass. The release of the cytotoxic CD8+ T cells into the circulation could exaberate the observed increase in ischemic injury. Finally, intravenous injection of human umbilical cord blood cells after MCAO stroke was shown to preserve the splenic mass likely via inhibition of CD8+ T cell release (Vendrame, et al., 2006). While such intriguing work has been completed to evaluate the potential interaction between progenitor cells and splenocytes in MCAO stroke models, we are not aware of any published studies that examined the effect of progenitor cells on splenocytes in a TBI model.

Using a CCI injury model for TBI creates localized parenchymal inflammation and edema thereby making injury cavity analysis a poor measure of therapeutic efficacy in the acute phase after injury. Therefore, Evan's blue dye extravasation was used to measure BBB permeability at the known temporal peak of cerebral edema development. BBB permeability increased 72 hours after injury in the CCI injury control animals (figure 2). Furthermore, the increase in permeability correlates with a significant reduction in splenic mass (figure 5A). The intravenous injection of both $2 * 10^6$ MAPC/kg $10 * 10^6$ MAPC/kg prevents the loss in splenic mass and maintain the integrity of the BBB. The same protocol repeated in animals after splenectomy failed to show such a dramatic increase in BBB permeability for CCI injury control animals indicating the spleen to be intimately involved in BBB breakdown. In addition, the spleen has to be present in order for the injected progenitor cells to have effect on BBB permeability.

To further characterize the loss in splenic mass, we completed flow cytometric based immunophenotyping of the cell surface markers, CD3, CD4, and CD8. Figure 5B outlines a significant increase in the percentage of CD3+/CD4+ double positive T cells. In accordance with the observed preservation of splenic mass, an absolute increase in the number of CD4+ T cells is present in the spleens of treatment animals. Additionally, figure 10A shows an increase in actively proliferating CD4+ T cells in the treatment groups indicating that the progenitor cell/splenocyte interaction is activating the resident T cells to proliferate accounting for the observed protection of splenic mass.

CD4+ T cells may differentiate into regulator or effector T cells that are responsible for many functions including modulation of the immunologic response and the release of anti inflammatory cytokines. Figure 10B shows a trend towards increased IL-4 and IL-10 production that reaches significance at the higher MAPC dosage ($10 * 10^6$ MAPC/kg). These findings represent a global increase in anti inflammatory cytokine production that could modulate the immunologic/inflammatory response and modulate the parenchymal and vascular tissue surrounding the area of injury leading to decreased resident endothelial cell and neuronal apoptosis thereby potentially attenuating the deficit observed with TBI.

Previous work completed by Pati et al. has shown preservation of the BBB with intravenous MSC therapy after TBI in a rat model. The effect was shown to be due to stabilization of the adherens junctions and proteins such as ve-cadherin and beta catenin. Therefore, we used occludin as a surrogate tight junction adherens protein as a surrogate marker for cerebral vasculature membrane integrity (Pati, et al.). Immunohistochemical images of the endothelial tight junction protein, occludin, evaluated the integrity of the BBB (figures 3 and 4). Occludin staining decreased in the CCI injury alone control animals. Additionally, the vessels present appear smaller and more disorganized. Occludin staining increased for both MAPC doses with elongation of the vasculature observed for the higher dosage ($10 * 10^6$ MAPC/kg). Furthermore, repeat staining with rats after splenectomy failed to show a qualitative difference in occludin staining when compared to uninjured control animals. This finding correlates well with the BBB permeability assay and further confirms the role of the spleen in the systemic inflammatory and injury response leading to BBB breakdown.

Analysis of the cortical sections confirmed that the most significant changes in the cerebral microvasculature occur in close proximity to the injury cavity edge.

Conclusions

While initial work investigating the potential role of progenitor cell therapeutics for TBI has shown great promise, the mechanism of action remains elusive. Our data show that TBI is associated with a reduction in splenic mass that correlates with the release of CD8+ lymphocytes that is associated with increased BBB permeability. The intravenous injection of MAPC preserves the BBB and splenic mass. Furthermore, the interaction between transplanted MAPC and resident CD4+ splenocytes leads to a global increase in IL-4 and IL-10 production that is a potential modulator of the cerebral microvasculature.

The functional end point of BBB preservation is observed for both cell dosages; however, further work to optimize cell dosing and timing is needed. A plausible hypothesized mechanism is that MAPC/splenocyte interactions generate anti-inflammatory cytokines and alter the splenocyte efflux in a manner that changes the endogenous cerebral inflammatory response. Overall, our data are consistent with other recent work indicating that injected progenitor cells do not need to engraft to produce a significant biological effect. In fact, injected progenitor cells could potentially act as “distant bioreactors” that modulate the systemic immunologic and inflammatory response via interactions with other organ systems such as splenocytes.

Acknowledgments

Supported by grants: NIH T32 GM 08 79201; M01 RR 02558; Texas Higher Education Coordinating Board; Children's Memorial Hermann Hospital Foundation; Texas Emerging Technology Fund; Athersys, Inc.

References

Consensus conference Rehabilitation of persons with traumatic brain injury. NIH Consensus Development Panel on Rehabilitation of Persons With Traumatic Brain Injury. JAMA. 1999; 282:974–983. [PubMed: 10485684]

Ajmo CT Jr, Collier LA, Leonardo CC, Hall AA, Green SM, Womble TA, Cuevas J, Willing AE, Pennypacker KR. Blockade of adrenoreceptors inhibits the splenic response to stroke. Exp Neurol. 2009; 218:47–55. [PubMed: 19371742]

Boozer S, L N, Lakshmipathy U, Love B, Raber A, Maitra A, Deans R, Rao MS, Ting AE. Global characterization and genomic stability of human multistem, A multipotent adult progenitor cell. Journal of Stem Cells. 2009; 4:17–28. [PubMed: 20498688]

Castro RF, Jackson KA, Goodell MA, Robertson CS, Liu H, Shine HD. Failure of bone marrow cells to transdifferentiate into neural cells in vivo. Science. 2002; 297:1299. [PubMed: 12193778]

Cotton BA, Snodgrass KB, Fleming SB, Carpenter RO, Kemp CD, Arbogast PG, Morris JA Jr. Beta-blocker exposure is associated with improved survival after severe traumatic brain injury. J Trauma. 2007; 62:26–33. discussion 33-25. [PubMed: 17215730]

Deng J, Petersen BE, Steindler DA, Jorgensen ML, Laywell ED. Mesenchymal stem cells spontaneously express neural proteins in culture and are neurogenic after transplantation. Stem Cells. 2006; 24:1054–1064. [PubMed: 16322639]

English D, Klasko SK, Sanberg PR. Elusive mechanisms of “stem cell”-mediated repair of cerebral damage. Exp Neurol. 2006; 199:10–15. [PubMed: 16730352]

Faul M, Wald MM, Rutland-Brown W, Sullivent EE, Sattin RW. Using a cost-benefit analysis to estimate outcomes of a clinical treatment guideline: testing theBrain Trauma Foundation guidelines for the treatment of severe traumatic brain injury. J Trauma. 2007; 63:1271–1278. [PubMed: 18212649]

Fischer UM, Harting MT, Jimenez F, Monzon-Posadas WO, Xue H, Savitz SI, Laine GA, Cox CS Jr. Pulmonary passage is a major obstacle for intravenous stem cell delivery: the pulmonary first-pass effect. Stem Cells Dev. 2009; 18:683–692. [PubMed: 19099374]

Harting MT, Jimenez F, Adams SD, Mercer DW, Cox CS Jr. Acute, regional inflammatory response after traumatic brain injury: Implications for cellular therapy. Surgery. 2008; 144:803–813. [PubMed: 19081024]

Harting MT, Jimenez F, Cox CS Jr. The pulmonary first-pass effect, xenotransplantation and translation to clinical trials--a commentary. Brain. 2008; 131:e100. author reply e101. [PubMed: 18669489]

Harting MT, Jimenez F, Xue H, Fischer UM, Baumgartner J, Dash PK, Cox CS. Intravenous mesenchymal stem cell therapy for traumatic brain injury. J Neurosurg. 2009; 110:1189–1197. [PubMed: 19301973]

Jiang Y, Vaessen B, Lenvik T, Blackstad M, Reyes M, Verfaillie CM. Multipotent progenitor cells can be isolated from postnatal murine bone marrow, muscle, and brain. Exp Hematol. 2002; 30:896–904. [PubMed: 12160841]

Liao W, Xie J, Zhong J, Liu Y, Du L, Zhou B, Xu J, Liu P, Yang S, Wang J, Han Z, Han ZC. Therapeutic effect of human umbilical cord multipotent mesenchymal stromal cells in a rat model of stroke. Transplantation. 2009; 87:350–359. [PubMed: 19202439]

Lighthall JW. Controlled cortical impact: a new experimental brain injury model. J Neurotrauma. 1988; 5:1–15. [PubMed: 3193461]

Lim JH, Byeon YE, Ryu HH, Jeong YH, Lee YW, Kim WH, Kang KS, Kweon OK. Transplantation of canine umbilical cord blood-derived mesenchymal stem cells in experimentally induced spinal cord injured dogs. J Vet Sci. 2007; 8:275–282. [PubMed: 17679775]

Offner H, Subramanian S, Parker SM, Afentoulis ME, Vandenbark AA, Hurn PD. Experimental stroke induces massive, rapid activation of the peripheral immune system. J Cereb Blood Flow Metab. 2006; 26:654–665. [PubMed: 16121126]

Offner H, Subramanian S, Parker SM, Wang C, Afentoulis ME, Lewis A, Vandenbark AA, Hurn PD. Splenic atrophy in experimental stroke is accompanied by increased regulatory T cells and circulating macrophages. J Immunol. 2006; 176:6523–6531. [PubMed: 16709809]

Pati S, Khakoo AY, Zhao J, Jimenez F, Gerber M, Harting MT, Redell JB, Grill RJ, Matsuo Y, Guha S, Cox CS, Reitz MS, Holcomb JB, Dash PK. Human mesenchymal stem cells inhibit vascular permeability by modulating VE-cadherin/beta-catenin signaling. Stem Cells Dev.

Qu C, Mahmood A, Lu D, Goussev A, Xiong Y, Chopp M. Treatment of traumatic brain injury in mice with marrow stromal cells. Brain Res. 2008; 1208:234–239. [PubMed: 18384759]

Schrepfer S, Deuse T, Reichenspurner H, Fischbein MP, Robbins RC, Pelletier MP. Stem cell transplantation: the lung barrier. Transplant Proc. 2007; 39:573–576. [PubMed: 17362785]

Thurman DJ, Alverson C, Dunn KA, Guerrero J, Sniezek JE. Traumatic brain injury in the United States: A public health perspective. J Head Trauma Rehabil. 1999; 14:602–615. [PubMed: 10671706]

Vendrame M, Gemma C, Pennypacker KR, Bickford PC, Davis Sanberg C, Sanberg PR, Willing AE. Cord blood rescues stroke-induced changes in splenocyte phenotype and function. Exp Neurol. 2006; 199:191–200. [PubMed: 16713598]

Walker PA, Shah SK, Harting MT, Cox CS. Progenitor cell therapies for traumatic brain injury: barriers and opportunities in translation. Dis Model Mech. 2009; 2:23–38. [PubMed: 19132123]

Zhao LR, Duan WM, Reyes M, Keene CD, Verfaillie CM, Low WC. Human bone marrow stem cells exhibit neural phenotypes and ameliorate neurological deficits after grafting into the ischemic brain of rats. Exp Neurol. 2002; 174:11–20. [PubMed: 11869029]

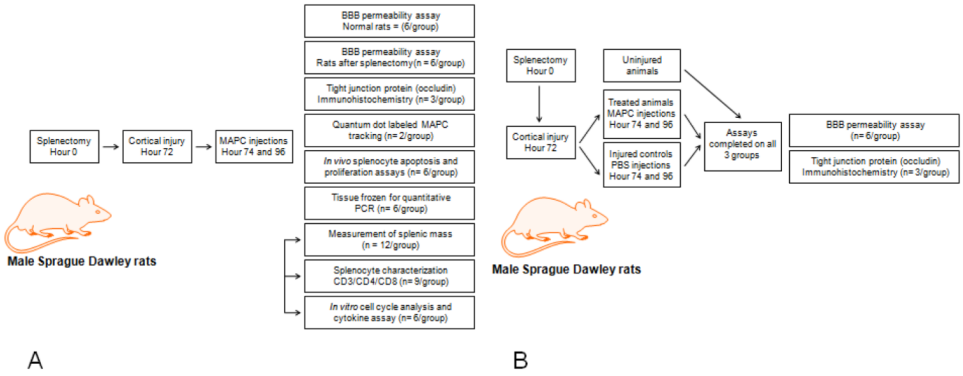

Figure 1.

(A) Experimental design for our experiments outlining the protocols and number of animals completed. The arrows connecting the protocols for splenocyte characterization, measurement of splenic mass, and *in vitro* cultures indicate that the same animals were used for the completion of all three protocols. **(B)** Experimental design for our experiments using animals after splenectomy outlining the protocols and number of animals completed.

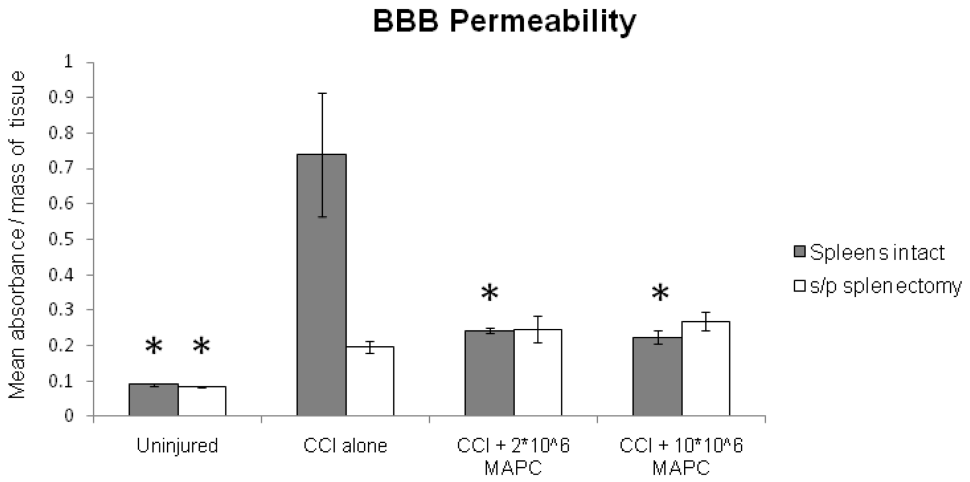

Figure 2.

Blood brain barrier (BBB) permeability measured via Evan's blue extravasation. BBB permeability measurement (mean absorbance/mg tissue) from homogenized cortical tissue derived from the hemisphere ipsilateral to CCI injury (n = 6/group). Increased BBB permeability is observed in normal rats after cortical injury with preservation towards uninjured levels with MAPC therapy. The same experiment completed in animals after splenectomy failed to show the increase in BBB permeability with cortical injury. Y axis represents mean absorbance normalized with mass of parenchymal tissue. * indicates statistical significance compared to CCI injury alone control sample (ANOVA with Tukey Kramer post hoc, $p < 0.05$).

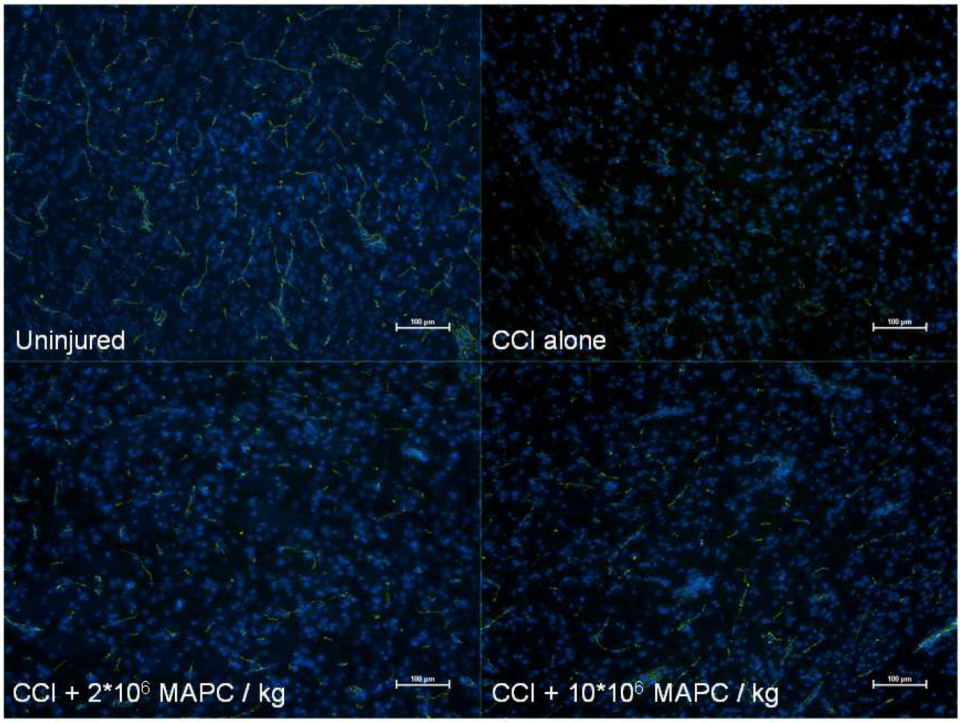

Figure 3.

Immunohistochemistry of the vascular architecture in the peri-lesion area of normal rats. Immunohistochemistry analyzing the tight junction protein occludin (FITC/green) with double stained nuclei (DAPI/blue). Observation of the slides shows a clear decrease in occludin staining in the CCI injury control animals when compared to the uninjured control group. Additionally, there appears to be an increase in occludin observed for both treatment groups. Close observation of the CCI + 2 * 10^6 MAPC/kg treatment group shows an increased occludin signal; however, the vasculature appears to be shorter and more disorganized than the uninjured controls. Furthermore, analysis of the CCI + 10 * 10^6 MAPC/kg treatment group shows both increased occluding staining and a larger population of more lengthy and organized vessels. (Pictures are 10× with bars measuring 100 μm).

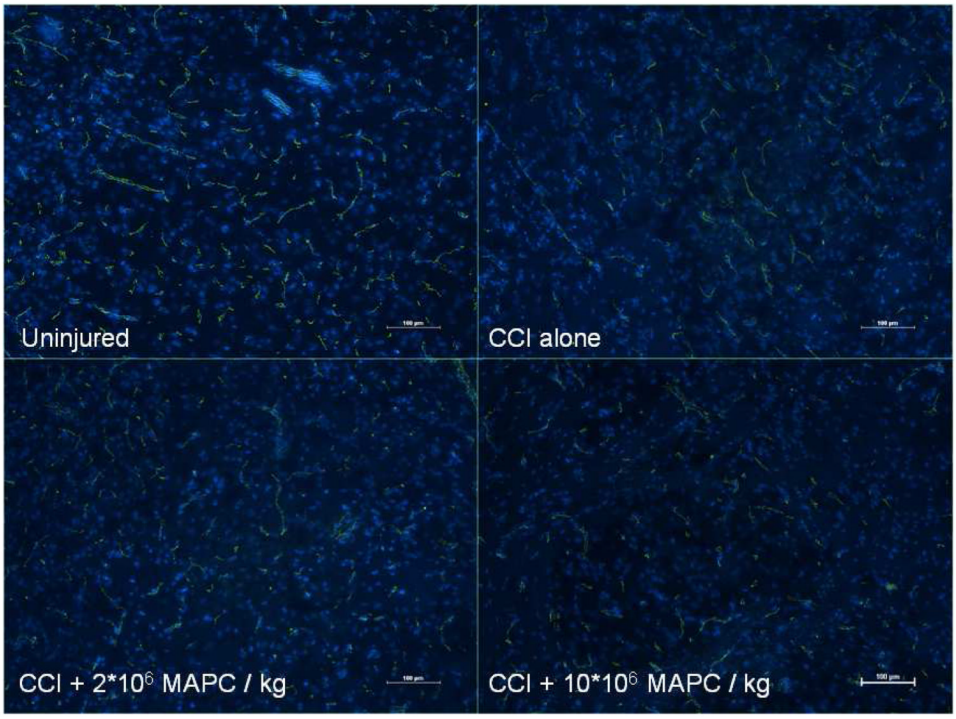

Figure 4.
Immunohistochemistry of the vascular architecture in the peri-lesion area of rats after splenectomy. Immunohistochemistry analyzing the tight junction protein occludin (FITC/green) with double stained nuclei (DAPI/blue) of rats status post splenectomy. Observation of the slides shows a slight decrease in occludin staining in the CCI injury control and treatment animals when compared to the uninjured control group. The observed difference is less pronounced than in the normal rats. Additionally, no clear difference in occludin staining is observed between the CCI injury alone and treatment groups. (Pictures are 10× with bars measuring 100 μm).

A

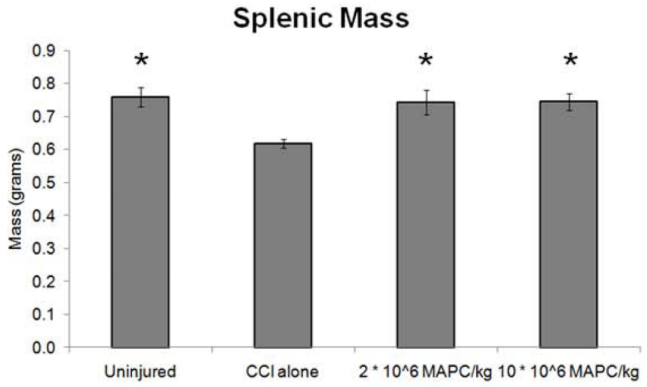

B

	Uninjured	CCI alone	CCI + 2 * 10^6 MAPC	CCI + 10 * 10^6 MAPC
CD3+ / CD4+	18.6 +/_ 0.80	16.9 +/_ 0.93	21.4 +/_ 0.57	24.2 +/_ 1.1*
CD3+ / CD8+	11.2 +/_ 0.43	11.2 +/_ 0.83	13.5 +/_ 0.75	13.0 +/_ 0.71
CD4+ / CD8+	0.61 +/_ 0.04	0.61 +/_ 0.08	0.63 +/_ 0.03	0.55 +/_ 0.05
CD200+	57.0 +/_ 0.80	55.3 +/_ 2.96	53.4 +/_ 2.35	54.9 +/_ 0.67
CD11	48.7 +/_ 3.94	55.8 +/_ 4.71	51.0 +/_ 1.05	56.2 +/_ 2.45

Figure 5.

Mass of spleens and splenocyte T cell characterization recorded 72 hours after cortical injury. **A)** Mass of spleens (grams) recorded 72 hours after CCI injury (n = 12/group). **B)** The percentage of splenocytes that were CD3+/CD4+ or CD3+/CD8+ double positive as well as the CD8+/CD4+ ratio (n = 9/group). A trend towards increased CD3+/CD4+ double positive cells was observed that reaches significance at the higher (10 * 10^6 MAPC/kg) cell dosage ($p < 0.001$). * indicates statistical significance compared to CCI injury alone control sample (ANOVA with Tukey Kramer post hoc $p < 0.05$).

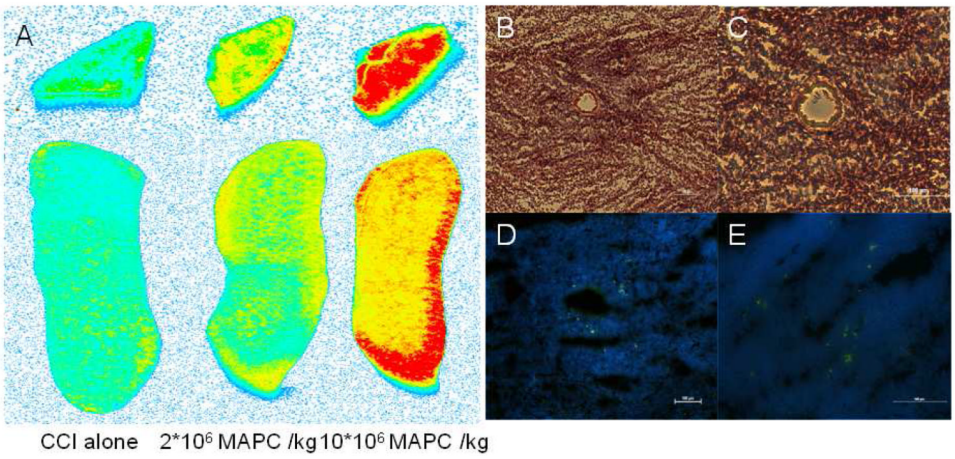

Figure 6.

In vivo tracking of quantum dot labeled MAPC after intervenous injection showing accumulation of cells in the spleen. Fluroescent scans (A), hematoxylin and eosin (H & E) structural stains (B - C), and immuno histochemistry (D - E) of quantum dot labeled (green) MAPCs located in splenic tissue. (A): Fluorescent scan of both total splenic body and splenic cross section to display the amount of MAPCs located in the spleen. As expected no signal (blue) is observed in the CCI alone control group. Further observation shows increasing signal (yellow representing a moderate signal and red representing a high level of signal) for both of the treatment groups indicating an increasing number of MAPCs located in within the splenic tissue. (B - C): H & E stain of a splenic cross section. Both images show a perforating arteriole within the splenic tissue. It is important to note that the splenic white pulp (areas rich in lymphocytes) are located around the arterioles. (D - E) shows several quantum dot labeled MAPCs (labeled green) located within the white pulp in close approximation with the blood vessel allowing for interaction with the resident splenic lymphocyte population. (B/D are 10× with bars measuring 100 μm) (C/E are 20× with bars measuring 100 μm).

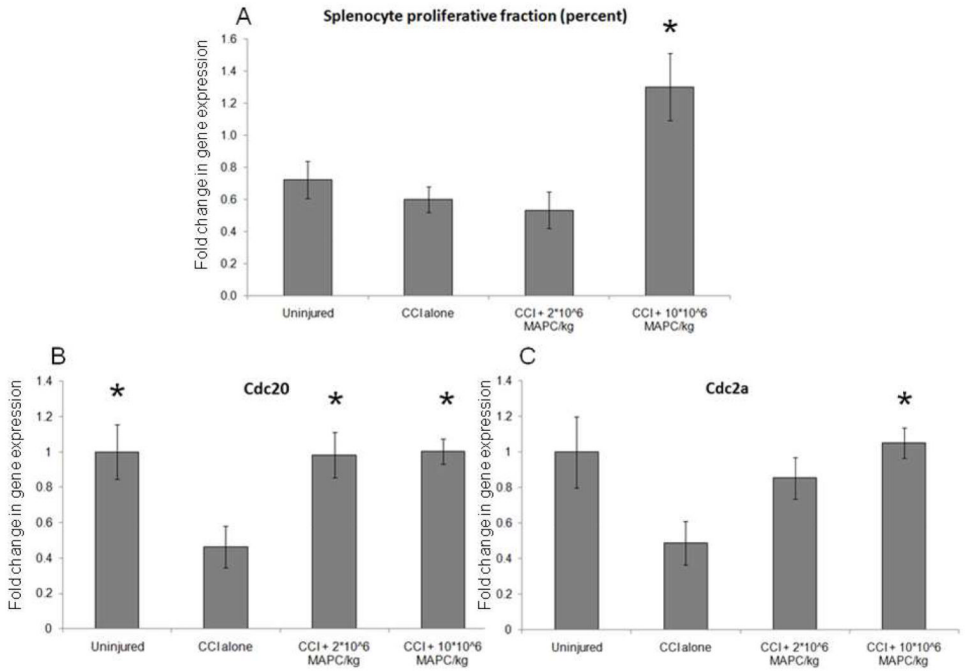

Figure 7.

(A) A significant increase in splenocyte proliferation at the higher MAPC dose (1.30 +/− 0.21%) when compared to CCI injury control animals (0.60 +/− 0.08%) ($p = 0.002$). **(B-C)** Significant increases in Cdc 20 expression for both treatment groups ($p = 0.01$) and in Cdc 2a expression for the higher ($10 * 10^6$ MAPC/kg) treatment group ($p = 0.03$) when compared to CCI injury controls. Values are expressed as fold increase from uninjured controls which are set to a value of 1.

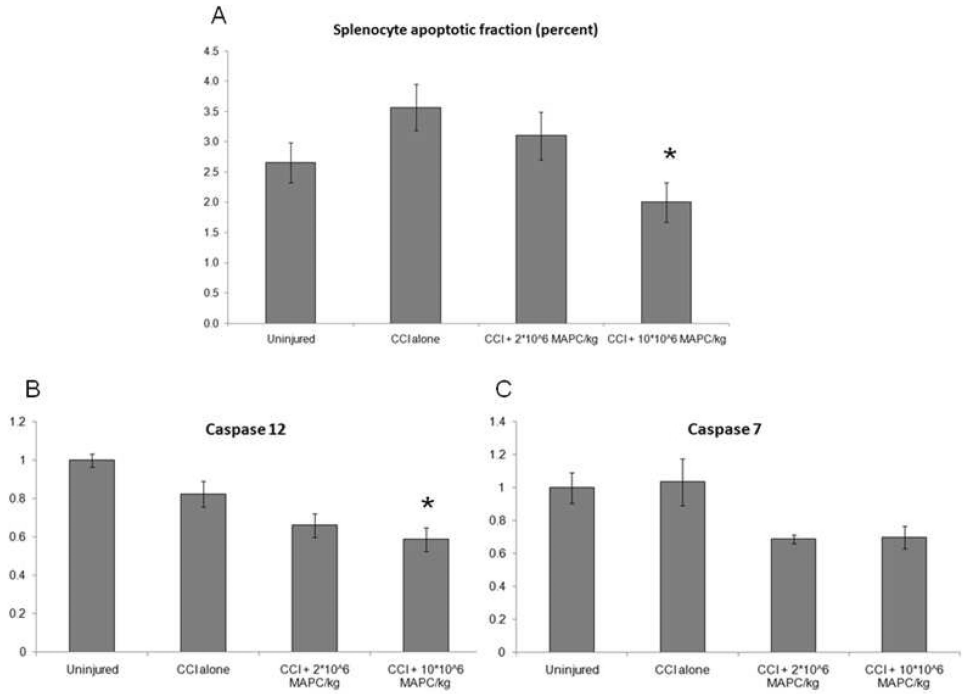

Figure 8.

(A) A significant decrease in splenocyte apoptosis at the higher MAPC dose (2.00 +/ −0.33%) when compared to CCI injury control animals (3.57 +/− 0.38%) ($p = 0.03$) via Annexin V staining. **(B)** A significant decrease in caspase 12 expression for the higher ($10 * 10^6$ MAPC/kg) treatment group ($p < 0.001$) when compared to CCI injury controls. **(C)** A decrease in caspase 7 expression for both treatment groups that fails to reach significance by post hoc analysis ($p = 0.02$). Values are expressed as fold increase from uninjured controls which are set to a value of 1.

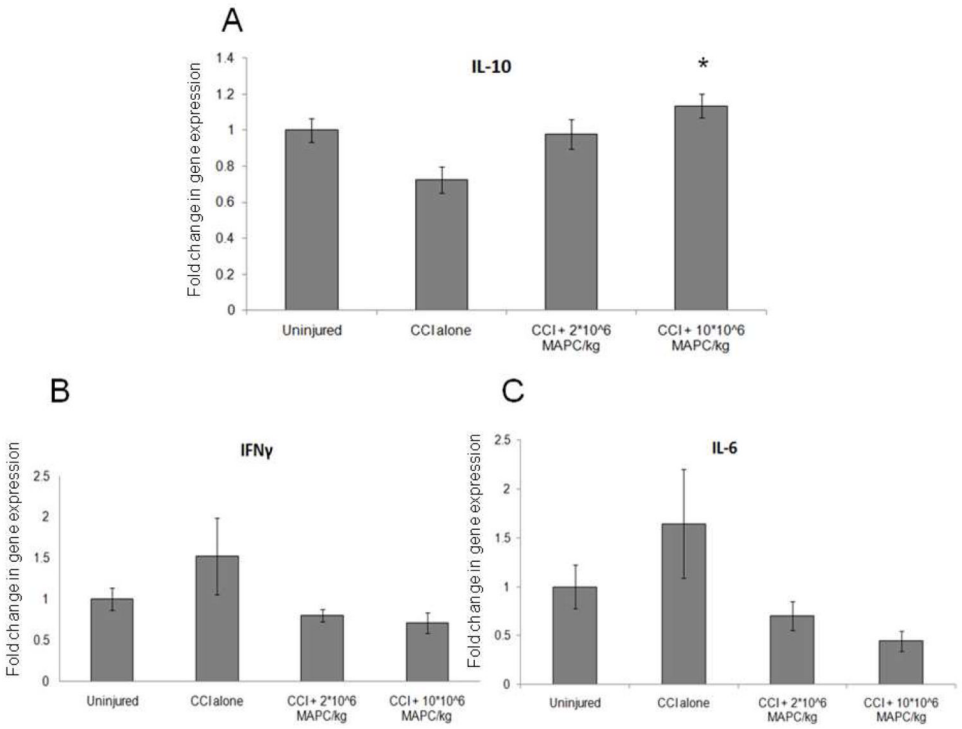

Figure 9.

(A) A significant increase in anti inflammatory cytokine (IL-10) production at the higher MAPC dose ($10 * 10^6$ MAPC/kg) when compared to CCI injury control animals ($p = 0.006$). **(B-C)** show a decrease in production of the pro inflammatory cytokines IL-6 and IFNγ that fails to reach significance ($p = 0.07$ and $p = 0.14$, respectively). Values are expressed as fold increase from uninjured controls which are set to a value of 1.

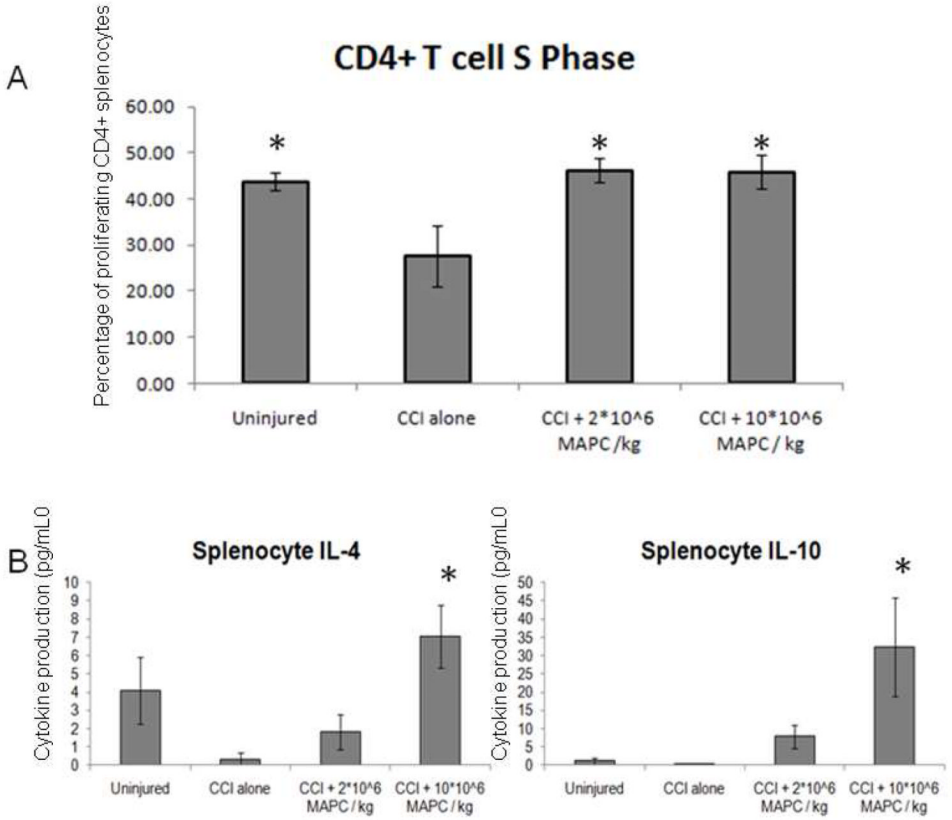

Figure 10.

Splenocyte CD4+ T cell proliferation and anti inflammatory cytokine production. **A)** Percentage of CD4+ splenocytes (n=6/group) that were in the S phase (actively proliferating). Control animals with CCI injury had a decrease in proliferation that was restored by both treatment doses. **B)** Anti inflammatory cytokine production (pg/mL) derived from splenocytes after 72 hours of expansion in stimulated (2 μg/mL) concanavalin A growth media. A trend towards increased cytokine production is observed for both cell doses. The trend reaches significance at the higher dose ($10 * 10^6$ MAPC/kg) for both IL-4 ($p = 0.02$) and IL-10 ($p = 0.03$) production. * indicates statistical significance compared to CCI injury alone control sample (ANOVA with Tukey Kramer post hoc, $p < 0.05$).

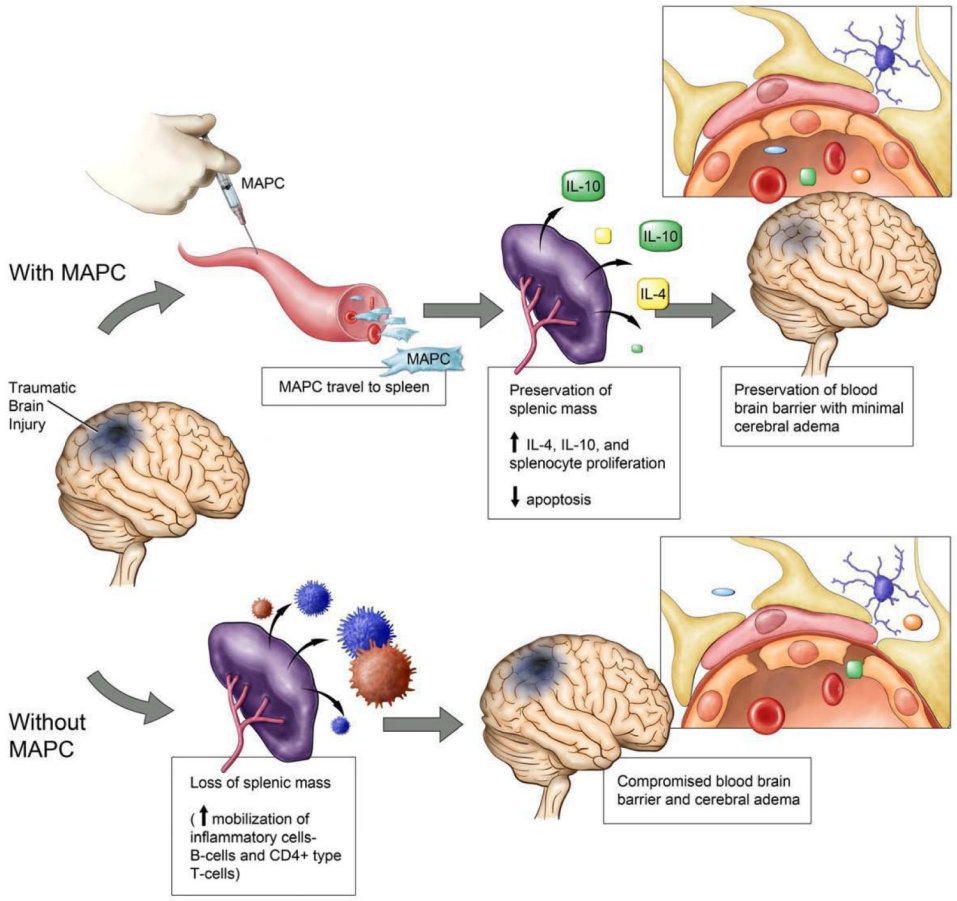

Figure 11.

Mechanism of neurovascular protection after the intravenous injection of MAPC. Our data show that CCI injury results in a decreased splenic mass and an increase in BBB permeability. Intravenous MAPC therapy preserved splenic mass and returned BBB permeability towards sham levels at both cell dosages. MAPC therapy leads to an increase in CD4+ splenocyte proliferation thereby increasing the production of anti inflammatory cytokines. The observed modulation of the inflammatory response causes stabilization of the cerebral microvasculature leading to the preservation of the BBB.

Table 1

List of forward and reverse primer sequences for the pro inflammatory cytokines interferon gamma (IFNγ) and interleukin 6 (IL-6), anti inflammatory cytokine interleukin 10 (IL-10), proliferative genes Cdc 20 and Cdc 2a, and apoptosis genes caspase 7 and caspase 12 used for quantitative PCR.

Transcript	Forward Primer	Reverse Primer
IFNγ	AACAGTAAAGCAAAAAAGGATGCA	TGCTGGATCTGTGGGTTGTTC
IL6	TCAACTCCATCTGCCCTTCAG	AAGGCAACTGGCTGGAAGTCT
IL10	GCCTTGTCAGAAATGATCAAGTTTT	TTTCTGGGCCATGGTTCTCT
Cdc20	GCCCATCCCCAATGCA	GCTGGGCCTGTGGCTTCT
Cdc2a	CAGAGCTGGCGACCAAGAA	AAGATCCTGAAGAGCTGGTCAATC
Casp7	CCATATCCACCAGCGCCTTA	GGTTCCCAGGGCCTCACTAG
Casp12	TCCTCCGACAGCACATTCCT	TGCTTCACCCCACAGATTCC
β-actin	AGCCCCCTCTGAACCCTAAG	CAACACAGCCTGGATGGCTAC